ACS Energy LETTERS

Cite This: ACS Energy Lett. 2019, 4, 1427−1431

http://pubs.acs.org/journal/aelccp

LETTER

CO_2 Electroreduction from Carbonate Electrolyte

Yuguang C. Li,[†,§] Geonhui Lee,[†,§] Tiange Yuan,[‡] Ying Wang,[†] Dae-Hyun Nam,[†] Ziyun Wang,[†] F. Pelayo García de Arquer,[†] Yanwei Lum,[†] Cao-Thang Dinh,[†] Oleksandr Voznyy,[‡] and Edward H. Sargent*[,†]

[†]Department of Electrical and Computer Engineering, University of Toronto, 35 St. George Street, Toronto, Ontario M5S 1A4, Canada

[‡]Department of Physical & Environmental Sciences, University of Toronto Scarborough, 1065 Military Trail, Toronto, Ontario M1C 1A4, Canada

Supporting Information

ABSTRACT: **The process of CO_2 valorization—from capture of CO_2 to its electrochemical upgrade—requires significant inputs in each of the capture, upgrade, and separation steps. Here we report an electrolyzer that upgrades carbonate electrolyte from CO_2 capture solution to syngas, achieving 100% carbon utilization across the system. A bipolar membrane is used to produce proton in situ to facilitate CO_2 release at the membrane:catalyst interface from the carbonate solution. Using a Ag catalyst, we generate syngas at a 3:1 H_2:CO ratio, and the product is not diluted by CO_2 at the gas outlet; we generate this pure syngas product stream at a current density of 150 mA/cm^2 and an energy efficiency of 35%. The carbonate-to-syngas system is stable under a continuous 145 h of catalytic operation. The work demonstrates the benefits of coupling CO_2 electrolysis with a CO_2 capture electrolyte on the path to practicable CO_2 conversion technologies.**

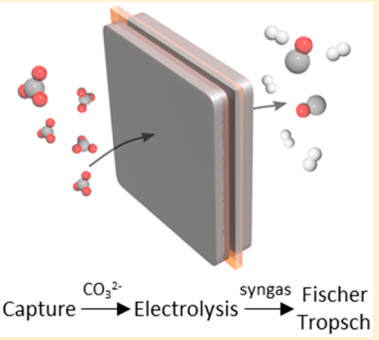

CO_2 capture systems often use alkali hydroxide solution to form alkali carbonate, and this requires additional energetic steps to dry and calcite the carbonate salt to generate a pure gas-phase CO_2 stream for the subsequent electrolysis reaction.[1,2] Direct electrochemical reduction of carbonate from the CO_2 capture solution could bypass the energy-intensive calcination step and reduce the carbon footprint of the CO_2-to-products process.

Such an approach would also address a limitation in present-day CO_2RR systems: the waste of CO_2 due to the conversion of CO_2 gas into carbonate anions, especially in alkaline solutions.[3,4] Carbonate anions travel through an anion exchange membrane (AEM), along with some CO_2RR products, and are oxidized at the anode.[5] Additionally, as much as 80% of the input CO_2 gas may simply exit the electrolysis cell unreacted: many systems exhibit low single-pass utilizations even along the input-to-output gas channel.[6,7] As illustrated in Figure 1a, with the loss of CO_2 due to carbonate formation, electrolyte crossover, and low single-pass conversion efficiency, the utilization of carbon is low in many present-day CO_2RR electrolyzer designs.

We focused herein on carrying out CO_2RR electrolysis using carbonate solution as the carbon supply. We document 100% carbon utilization of input-carbon-to-products, evidenced by the lack of gaseous CO_2 at the reactor outlet. We do so by levering the facile acid/base reaction between a proton and carbonate anion. We design an electrolysis system that generates CO_2 in situ from carbonate to initiate CO_2RR.

Figure 1b shows the conventional/prior catalyst−membrane approach that uses a membrane−electrode assembly (MEA) design.

Here we instead use a bipolar membrane (BPM), which consists of a catalyst layer to dissociate water to generate protons and hydroxide anions and directs them to the cathode and anode, respectively. The energy for water dissociation is recovered by lowering the Nernstian overpotential at the anode and cathode due to the pH gradient.[8−17] Carbonate electrolyte circulates to the cathode via a peristaltic pump. Under applied potential conditions, the BPM proton reacts with carbonate to generate CO_2 near the membrane:cathode interface (Figure 1b and Video S1), and this is reduced to value-added products via CO_2RR. The chemical balance is presented in Figure 1c.

We evaluated performance using Ag electrocatalysts (Figures S1 and S3) and Cu electrocatalysts (Figures S2 and S4) in 1 M K_2CO_3 electrolyte. The catholyte in Figure 2a−c was purged using N_2 to remove dissolved CO_2. Ni foam was used as the anode with 1 M KOH electrolyte, a nonprecious catalyst in an

Received: May 5, 2019
Accepted: May 24, 2019
Published: May 24, 2019

DOI: 10.1021/acsenergylett.9b00975
ACS Energy Lett. 2019, 4, 1427−1431

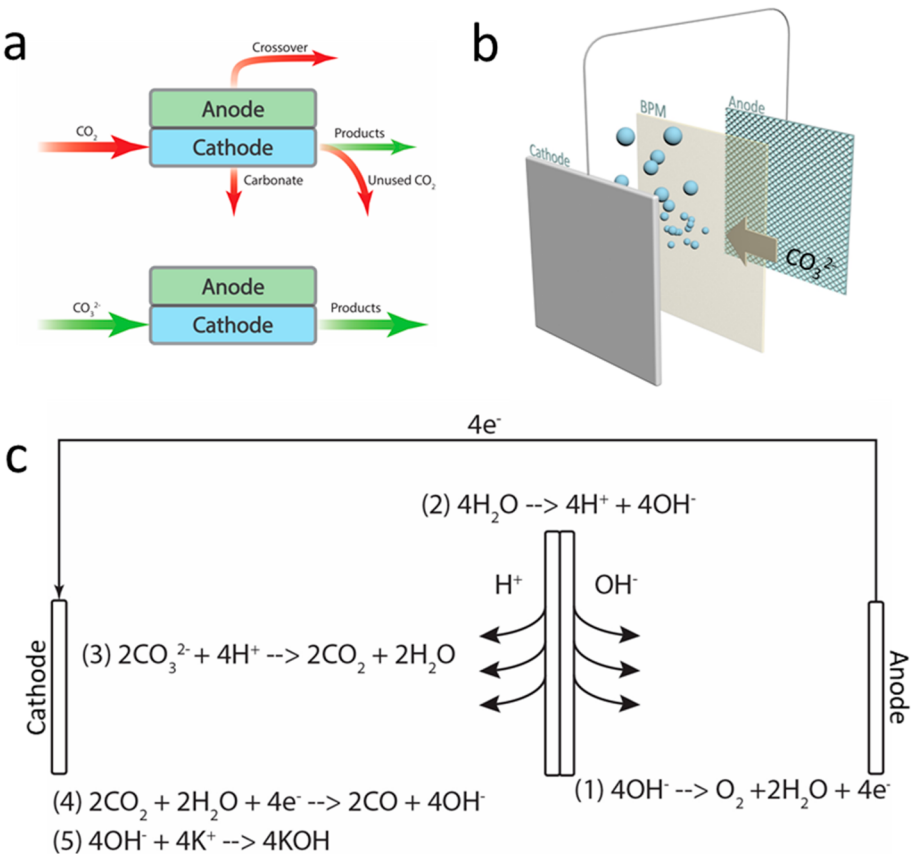

Figure 1. (a) Carbon loss mechanisms in a CO_2 electrolysis cell with gas-fed CO_2. (b) Illustration of the BPM generating CO_2 in situ via the acid/base reaction of the proton and carbonate ion. (c) Full chemical balance of the direct carbonate electrolysis cell with BPM.

alkaline condition, favorable for the oxygen evolution reaction. All studies herein report the full cell voltage, which includes the series resistance, transport, and kinetic overpotentials, from the cathode, anode, and membrane, as seen for example in Figure 2a. The onset full cell potentials for both Ag and Cu catalysts were observed at ca. 2.2 V, with Ag showing faster kinetics at higher applied potentials. For the Ag catalyst (Figure 2b), the CO Faradaic efficiency (FE) ranges from 28 to 12% at applied current densities of 100−300 mA/cm^2, with the remainder of the FE going to hydrogen. We carried out carbon-13 experiments that ascertained that CO_2RR products come from CO_2 and not contaminants (Figure S5). This yields a syngas ratio (H_2:CO) ranging from 2.5 to 7, suitable as feedstock to the Fischer−Tropsch (FT) reaction.[18] Because the source of carbon in this reaction is carbonate—a liquid phase reactant—the gas product exiting the electrolysis cell is pure syngas with a small amount of moisture. Gas chromatography confirms that no CO_2 is detected from the gas outlet stream. The full cell energy efficiency (EE) is 35% at 150 mA/cm^2, where in the product values we have included the contributions of both CO and H_2.

With a Cu catalyst, ca. 10% FE of ethylene is detected, as well as a small amount of ethanol and methane. In total, 17% CO_2RR to hydrocarbon products was achieved. The full product distribution is available in Table S1.

The BPM also offers the benefit of mitigating product crossover as a result of the electro-osmotic drag of protons emerging from the membrane, opposing the direction of product migration from the cathode to anode.[5,19] Anolytes from the Cu catalyst experiments were analyzed, and no liquid products were detected on the anode side. With this system design, carbon loss mechanisms in a typical flow cell are circumvented: CO_2 reaction with electrolyte to form carbonate; low single-pass CO_2 utilization; and product crossover in the AEM system.

We examined the compatibility of the carbonate electrolysis cell in different CO_2 capture solutions directly. CO_2 gas was bubbled into 0.1−2 M KOH solutions, simulating an industrial CO_2 capture process, and the CO_2-purged electrolyte was tested for carbonate electrolysis, shown in Figure 2d. The pH of the capture solution following CO_2 purging remained between 10 and 11 (Tables S2 and S3), which indicates that carbonate is the primary carbon species after CO_2 capture. During reaction, unreacted CO_2 exiting the membrane:catalyst interface will form carbonate again due to chemical equilibrium at this pH, and the carbonate ion will then be recycled for subsequent reaction. With a Ag catalyst, the CO FE performance was observed to increase in linear proportion with the concentration of the KOH electrolyte. This is ascribed to the increase of the capture-generated K_2CO_3 concentration. The best performance of the KOH−CO_2 capture electrolyte shows a few-percentage improvement compared to that of the pure K_2CO_3 electrolyte (Figure 2b). This is likely due to the small amount of bicarbonate salt present in the solution, which may generate a small amount of CO_2 via chemical equilibrium and also a small amount of dissolved CO_2, each giving additional sources of reactant.[20,21]

In the full system chemical balance provided in Figure 1c, carbonate is consumed as the source of carbon in the cathodic reaction, and hydroxide is generated from the reduction

DOI: 10.1021/acsenergylett.9b00975
ACS Energy Lett. 2019, 4, 1427−1431

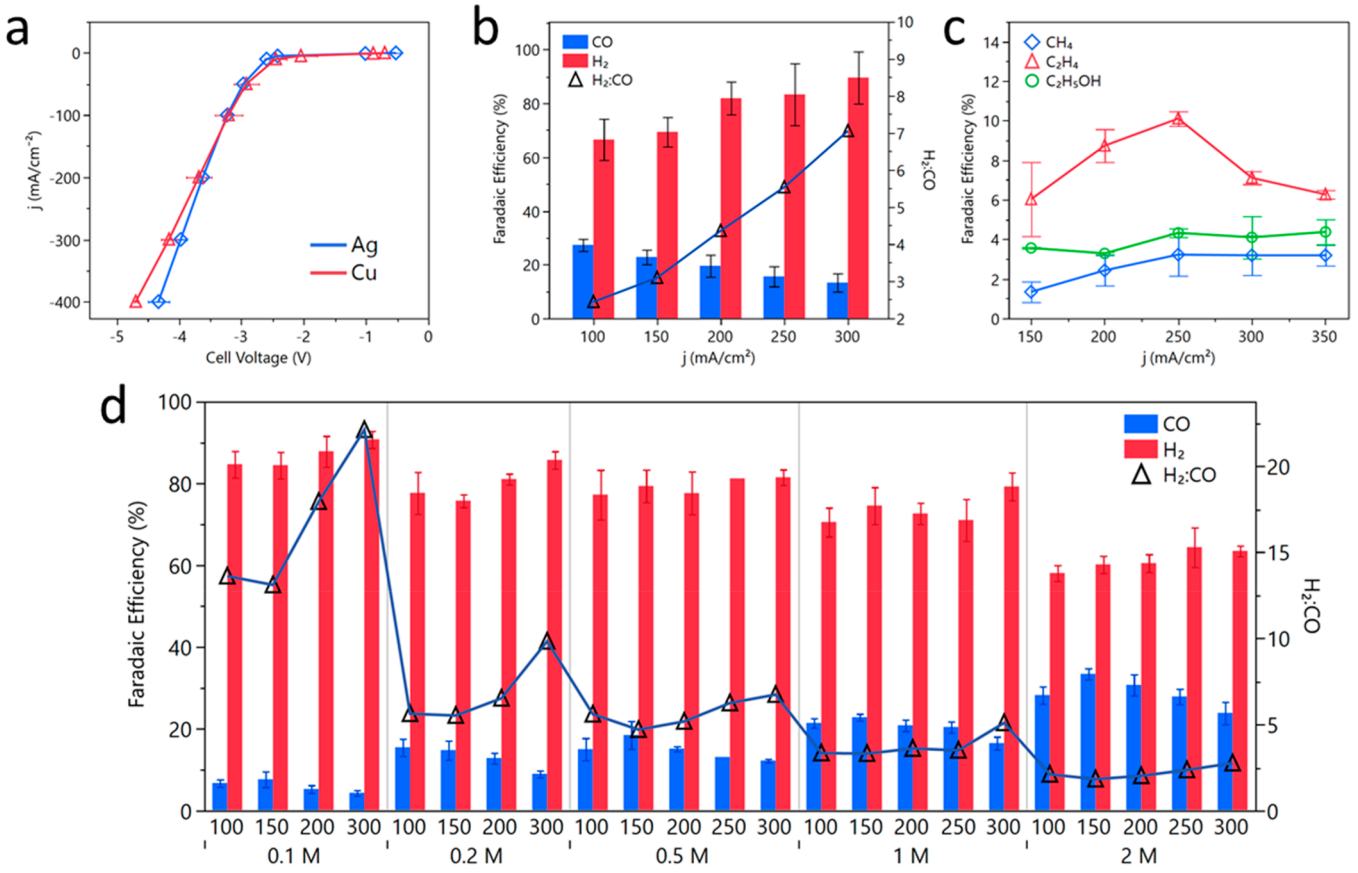

Figure 2. Performance of the carbonate electrolysis cell. (a) Full cell $j-V$ curve with Ag and Cu catalyst. (b) Product distribution for the Ag catalyst. H_2 and CO are the major products, summing up to ~100% of the total FE. (c) Product distribution for the Cu catalyst. Propanol, formate, and acetate are detected as well in a small amount. (a–c) Conducted in 1 M K_2CO_3 catholyte with nitrogen purging as controls to demonstrate the concept of in situ CO_2 generations; 1 M KOH and Ni foam were used at the anode. (d) Product distribution of a Ag catalyst under different applied current density (first x-axis, mA/cm^2) in different concentrations of KOH electrolyte (second x-axis) purged with CO_2 prior to reaction, simulating the product of a CO_2 capture solution.

reaction, as shown in previous studies;[22−25] this has the effect of regenerating the CO_2 capture solution.

The capture-and-electrolysis system is therefore capable of operating continuously: the KOH capture solution removes CO_2 from the air or flue gas, forming carbonate; the carbonate electrolyte is then reduced to form value-added products via electrolysis with high carbon utilization; and the capture solution is thereby regenerated to restart the cycle.

We demonstrate a capture−electrolysis system in continuous operation for 145 h with a Ag catalyst (in Figure 3). Two electrolyte bottles were used—one for capturing CO_2 gas directly with KOH electrolyte and a second one for electrolysis, where no gas purging is performed. The carbonate capture solution and the electrolysis electrolyte are exchanged using a peristaltic pump (Figure S6). The electrolyte in the electrolysis bottle is pumped to the carbonate cell with no gas purging. The pH values of the electrolysis bottle and the capture bottle are measured to monitor the KOH regeneration and system stability (Table S3). Syngas generated from the reaction exits the bottle to a mass flow meter. The flow rate of gas products was recorded to calculate the total gas produced. During the 145 h of electrolysis, the current density was stable at ca. 180 mA/cm^2, a reflection of the pH balance and crossover-prevention benefits offered by the BPM. The H_2:CO ratio also remained stable at between 2 and 3; small fluctuation of the ratio could be

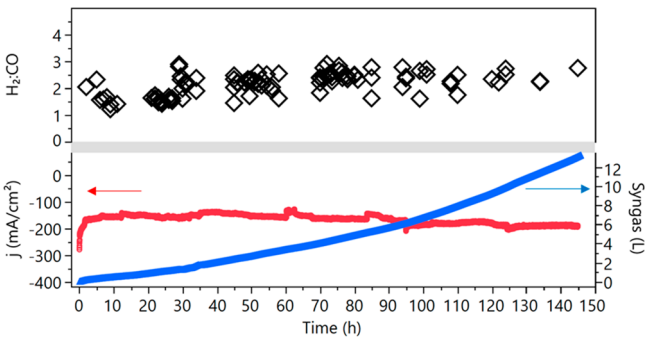

Figure 3. Stability evaluation of the carbonate electrolysis cell. CO_2 gas was first captured with KOH solution and transferred to an electrolysis bottle with no gas purging. The amount of gas produced from the electrolysis was measured with a mass flow meter, and the ratio of H_2 and CO was monitored with GC injection; 1 M KOH and Ni foam were used at the anode. The cell was held at a constant potential of 3.8 V.

accounted for by the contamination metal deposition overtime.[26] Approximately 13 L of syngas was collected.

To assess the economics of the carbonate reduction, we calculated the energy cost per product molecule, considering the process from CO_2 capture and electrolysis to separation processes, based on typical reported results from the literature at similar current densities. We evaluated:

DOI: 10.1021/acsenergylett.9b00975
ACS Energy Lett. 2019, 4, 1427−1431

- the alkaline flow cell[27−29]
- the MEA cell[7,30] with gas-fed CO_2
- the carbonate cell explored herein.

Table 1 summarizes the results (detailed calculations are available in the SI). The total energy required to generate 1 mol of products is 4 times higher in the MEA cell with gas-fed CO_2 and 6 times higher for the alkaline flow cell. The cost of capture and separation can vary depending on applications, and Figure 4 shows the energy capital per product molecule as a function of the CO_2 capture cost and the separation cost.[31−33] Even in the scenario of low capture cost and low separation cost, the energy cost for CO_2RR in today's gas-fed CO_2 MEA cells is about 2 times higher than that in the carbonate cell. Regeneration costs associated with removing carbonate from the electrolyte and from the anodic side add further to the expense of producing fuels and feedstocks in the gas-fed CO_2 MEA cell.

Table 1. Energy Cost for the Alkaline Flow Cell, CO_2 Gas-Fed MEA Cell and Carbonate Cell[a]

energy capital	flow cell	MEA	CO_3^{2-}
CO_2 utilization	10	20	100
carbonate formation (%)	38	0	0
crossover (%)	2	30	0
exit CO_2 (%)	50	50	0
CO_2 capture (kJ/mol product)	1783	892	0
CO_2 required (mol)	10	5	1
CO_2RR (kJ/mol product)	367	643	733
EE (%)	70	40	35
separation(kJ/mol)	2500	1250	0
energy/product (kJ/mol product)	4650	2785	733

[a]The cost of CO_2 capture was taken to be 178 kJ/mol,1 and the energy cost of separation is 500 kJ/mol.[31,32]

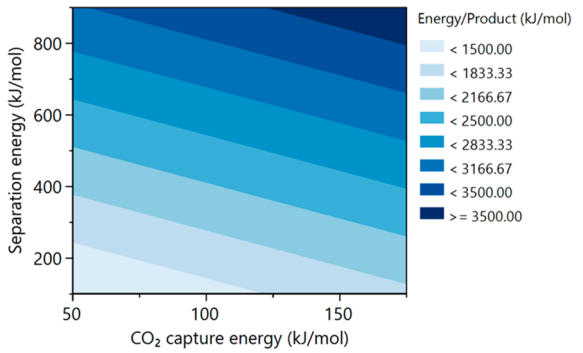

Figure 4. Technoeconomic analysis of the MEA cell with gas-fed CO_2 with different energy costs for CO_2 capture and different energy costs for product separation.

A number of topics require further study and progress in the carbonate cell. The thermodynamic onset potential for CO_2 reduction to syngas is approximately 1.34 V, and the experimental onset potential is ca. 2.2 V. The overpotential is large compared to that of a water electrolyzer, which obtains 1 A/cm^2 using less than 1 V of full cell overpotential.[34] Optimization of each cell component will be required, increasing the full cell EE further and thereby lowering the energy consumption associated with CO_2RR. A possible outcome is to generate substantially pure CO from carbonate and combine it with an industrial hydrogen source to further improve the overall efficiency. While the gas products generated in the carbonate electrolysis cell do not contain CO_2, moisture is present in the exit stream, and this will require separation before the syngas is utilized. There are also several competing reactions on the cathodic side. When a proton is generated from the BPM, it can be reduced directly on the cathode, leading to HER; when CO_2 is generated from carbonate, it can react with KOH, forming carbonate again, instead of being reduced in CO_2RR; and the proton from the BPM can also simply react with KOH in the electrolyte to form water. The penalties for these side reactions are reflected in less-than-100% total Faradaic efficiencies seen herein.

Another challenge for the carbonate cell is the acidic local environment at the membrane:catalyst interface due to proton generation from the BPM. The successful development of an acidic CO_2RR catalyst will further improve the FE and lead to better utilization of in situ-generated CO_2. The syngas reported herein provides H_2:CO in a 3:1 ratio, which is of industry interest,[35] but future studies of carbonate-to-products will benefit from further insights, progress, and innovation to a wider range of syngas ratios and, more beneficially still, to higher-value products in better conversion efficiency.

The system design herein achieves carbonate conversion via the acid/base reaction of the proton and carbonate, which generates an in situ source of CO_2, enabled by the use of a BPM. The device operated continuously for 145 h and generated syngas in a suitable ratio for subsequent FT reaction. A FE of 17% of the total carbonate-to-hydrocarbon products was also achieved with a Cu catalyst. This study demonstrates the direct implementation of carbonate to CO_2RR products from a CO_2 capture solution as the input and a gas product suitable for the FT reaction as the output. It enables the utilization of captured CO_2 to hydrocarbon products.

■ ASSOCIATED CONTENT

Supporting Information

The Supporting Information is available free of charge on the ACS Publications website at DOI: 10.1021/acsenergylett.9b00975.

Experimental details, supplementary Figures S1−S6 showing SEM images, XRD patterns, GC-MS analysis, and the experimental setup, and supplementary Table S1−S3 providing product distributions and electrolyte pH (PDF)

Video of the BPM proton reacting with carbonate to generate CO_2 near the membrane:cathode interface (AVI)

■ AUTHOR INFORMATION

Corresponding Author

*E-mail: ted.sargent@utoronto.ca.

ORCID

Yuguang C. Li: 0000-0002-9559-7051
Ying Wang: 0000-0002-6240-5535
Dae-Hyun Nam: 0000-0002-0871-1355
Ziyun Wang: 0000-0002-2817-8367
Cao-Thang Dinh: 0000-0001-9641-9815
Oleksandr Voznyy: 0000-0002-8656-5074
Edward H. Sargent: 0000-0003-0396-6495

DOI: 10.1021/acsenergylett.9b00975
ACS Energy Lett. 2019, 4, 1427−1431

Author Contributions

[§]Y.C.L. and G.L. contributed equally to this work.

Notes

The authors declare no competing financial interest.

■ ACKNOWLEDGMENTS

The authors would like to acknowledge funding support from the Canadian Institute for Advanced Research (CIFAR), the Ontario Research Fund-Research Excellence program, and the Natural Sciences and Engineering Research Council (NSERC).

■ REFERENCES

(1) Keith, D. W.; Holmes, G.; St. Angelo, D.; Heidel, K. A Process for Capturing CO_2 from the Atmosphere. *Joule* **2018**, *2* (8), 1573−1594.
(2) Sanz-Pérez, E. S.; Murdock, C. R.; Didas, S. A.; Jones, C. W. Direct Capture of CO_2 from Ambient Air. *Chem. Rev.* **2016**, *116* (19), 11840−11876.
(3) Dinh, C. T.; Burdyny, T.; Kibria, M. G.; Seifitokaldani, A.; Gabardo, C. M.; García de Arquer, F. P.; Kiani, A.; Edwards, J. P.; De Luna, P.; Bushuyev, O. S.; Zou, C.; Quintero-Bermudez, R.; Pang, Y.; Sinton, D.; Sargent, E. H. CO_2 Electroreduction to Ethylene via Hydroxide-mediated Copper Catalysis at an Abrupt Interface. *Science* **2018**, *360* (6390), 783.
(4) Lv, J.-J.; Jouny, M.; Luc, W.; Zhu, W.; Zhu, J.-J.; Jiao, F. A Highly Porous Copper Electrocatalyst for Carbon Dioxide Reduction. *Adv. Mater.* **2018**, *30* (49), 1803111.
(5) Li, Y. C.; Yan, Z.; Hitt, J.; Wycisk, R.; Pintauro, P. N.; Mallouk, T. E. Bipolar Membranes Inhibit Product Crossover in CO_2 Electrolysis Cells. *Adv. Sustainable Syst.* **2018**, *2* (4), 1700187.
(6) Dinh, C.-T.; Li, Y. C.; Sargent, E. H. Boosting the Single-Pass Conversion for Renewable Chemical Electrosynthesis. *Joule* **2019**, *3* (1), 13−15.
(7) Weng, L.-C.; Bell, A. T.; Weber, A. Z. Towards Membrane-Electrode Assembly Systems for CO_2 Reduction: A Modeling Study. *Energy Environ. Sci.* **2019**, DOI: 10.1039/C9EE00909D.
(8) Li, Y. C.; Zhou, D.; Yan, Z.; Gonçalves, R. H.; Salvatore, D. A.; Berlinguette, C. P.; Mallouk, T. E. Electrolysis of CO_2 to Syngas in Bipolar Membrane-Based Electrochemical Cells. *ACS Energy Lett.* **2016**, *1* (6), 1149−1153.
(9) Yan, Z.; Zhu, L.; Li, Y. C.; Wycisk, R. J.; Pintauro, P. N.; Hickner, M. A.; Mallouk, T. E. The Balance of Electric Field and Interfacial Catalysis in Promoting Water Dissociation in Bipolar Membranes. *Energy Environ. Sci.* **2018**, *11* (8), 2235−2245.
(10) Vermaas, D. A.; Smith, W. A. Synergistic Electrochemical CO_2 Reduction and Water Oxidation with a Bipolar Membrane. *ACS Energy Lett.* **2016**, *1* (6), 1143−1148.
(11) Salvatore, D. A.; Weekes, D. M.; He, J.; Dettelbach, K. E.; Li, Y. C.; Mallouk, T. E.; Berlinguette, C. P. Electrolysis of Gaseous CO_2 to CO in a Flow Cell with a Bipolar Membrane. *ACS Energy Lett.* **2018**, *3* (1), 149−154.
(12) Dai, J.; Dong, Y.; Gao, P.; Ren, J.; Yu, C.; Hu, H.; Zhu, Y.; Teng, X. A Sandwiched Bipolar Membrane for All Vanadium Redox Flow Battery with High Coulombic Efficiency. *Polymer* **2018**, *140*, 233−239.
(13) Ho, A.; Zhou, X.; Han, L.; Sullivan, I.; Karp, C.; Lewis, N. S.; Xiang, C. Decoupling $H_2(g)$ and $O_2(g)$ Production in Water Splitting by a Solar-Driven $V^{3+/2+}(aq,H_2SO_4)|KOH(aq)$ Cell. *ACS Energy Lett.* **2019**, *4* (4), 968−976.
(14) Luo, J.; Vermaas, D. A.; Bi, D.; Hagfeldt, A.; Smith, W. A.; Grätzel, M. Bipolar Membrane-Assisted Solar Water Splitting in Optimal pH. *Adv. Energy Mater.* **2016**, *6* (13), 1600100.
(15) McDonald, M. B.; Bruce, J. P.; McEleney, K.; Freund, M. S. Reduced Graphene Oxide Bipolar Membranes for Integrated Solar Water Splitting in Optimal pH. *ChemSusChem* **2015**, *8* (16), 2645−2654.
(16) Schreier, M.; Héroguel, F.; Steier, L.; Ahmad, S.; Luterbacher, J. S.; Mayer, M.; Luo, J.; Graetzel, M. Solar Conversion of CO_2 to CO Using Earth-Abundant Electrocatalysts Prepared by Atomic Layer Modification of CuO. *Nat. Energy* **2017**, *2*, 17087.
(17) Reiter, R. S.; White, W.; Ardo, S. Electrochemical Characterization of Commercial Bipolar Membranes under Electrolyte Conditions Relevant to Solar Fuels Technologies. *J. Electrochem. Soc.* **2016**, *163* (4), H3132−H3134.
(18) Klerk, A. d. Fischer−Tropsch Process. *Kirk-Othmer Encyclopedia of Chemical Technology*; 2013.
(19) Ramdin, M.; Morrison, A. R. T.; de Groen, M.; van Haperen, R.; de Kler, R.; van den Broeke, L. J. P.; Trusler, J. P. M.; de Jong, W.; Vlugt, T. J. H. High Pressure Electrochemical Reduction of CO_2 to Formic Acid/Formate: A Comparison between Bipolar Membranes and Cation Exchange Membranes. *Ind. Eng. Chem. Res.* **2019**, *58* (5), 1834−1847.
(20) Lee, C. H.; Kanan, M. W. Controlling H+ vs CO_2 Reduction Selectivity on Pb Electrodes. *ACS Catal.* **2015**, *5* (1), 465−469.
(21) Min, X.; Kanan, M. W. Pd-Catalyzed Electrohydrogenation of Carbon Dioxide to Formate: High Mass Activity at Low Overpotential and Identification of the Deactivation Pathway. *J. Am. Chem. Soc.* **2015**, *137* (14), 4701−4708.
(22) Weng, L.-C.; Bell, A. T.; Weber, A. Z. Modeling gas-diffusion electrodes for CO_2 reduction. *Phys. Chem. Chem. Phys.* **2018**, *20* (25), 16973−16984.
(23) Singh, M. R.; Kwon, Y.; Lum, Y.; Ager, J. W.; Bell, A. T. Hydrolysis of Electrolyte Cations Enhances the Electrochemical Reduction of CO_2 over Ag and Cu. *J. Am. Chem. Soc.* **2016**, *138* (39), 13006−13012.
(24) Gupta, N.; Gattrell, M.; MacDougall, B. Calculation for the Cathode Surface Concentrations in the Electrochemical Reduction of CO_2 in $KHCO_3$ Solutions. *J. Appl. Electrochem.* **2006**, *36* (2), 161−172.
(25) Burdyny, T.; Smith, W. A. CO2 Reduction on Gas-diffusion Electrodes and Why Catalytic Performance Must be Assessed at Commercially-relevant Conditions. *Energy Environ. Sci.* **2019**, *12* (5), 1442−1453.
(26) Hori, Y.; Konishi, H.; Futamura, T.; Murata, A.; Koga, O.; Sakurai, H.; Oguma, K. Deactivation of Copper Electrode" in Electrochemical Reduction of CO_2. *Electrochim. Acta* **2005**, *50* (27), 5354−5369.
(27) Verma, S.; Lu, X.; Ma, S.; Masel, R. I.; Kenis, P. J. A. The Effect of Electrolyte Composition on the Electroreduction of CO_2 to CO on Ag Based Gas Diffusion Electrodes. *Phys. Chem. Chem. Phys.* **2016**, *18* (10), 7075−7084.
(28) Verma, S.; Hamasaki, Y.; Kim, C.; Huang, W.; Lu, S.; Jhong, H.-R. M.; Gewirth, A. A.; Fujigaya, T.; Nakashima, N.; Kenis, P. J. A. Insights into the Low Overpotential Electroreduction of CO_2 to CO on a Supported Gold Catalyst in an Alkaline Flow Electrolyzer. *ACS Energy Lett.* **2018**, *3* (1), 193−198.
(29) Ma, S.; Luo, R.; Gold, J. I.; Yu, A. Z.; Kim, B.; Kenis, P. J. A. Carbon Nanotube Containing Ag Catalyst Layers for Efficient and Selective Reduction of Carbon Dioxide. *J. Mater. Chem. A* **2016**, *4* (22), 8573−8578.
(30) Kutz, R. B.; Chen, Q.; Yang, H.; Sajjad, S. D.; Liu, Z.; Masel, I. R. Sustainion Imidazolium-Functionalized Polymers for Carbon Dioxide Electrolysis. *Energy Technology* **2017**, *5* (6), 929−936.
(31) Ho, M. T.; Allinson, G. W.; Wiley, D. E. Reducing the Cost of CO_2 Capture from Flue Gases Using Pressure Swing Adsorption. *Ind. Eng. Chem. Res.* **2008**, *47* (14), 4883−4890.
(32) Aaron, D.; Tsouris, C. Separation of CO_2 from Flue Gas: A Review. *Sep. Sci. Technol.* **2005**, *40* (1−3), 321−348.
(33) Verma, S.; Lu, S.; Kenis, P. J. A. Co-electrolysis of CO_2 and Glycerol as a Pathway to Carbon Chemicals with Improved Technoeconomics Due to Low Electricity Consumption. *Nat. Energy* **2019**, DOI: 10.1038/s41560-019-0374-6.
(34) Carmo, M.; Fritz, D. L.; Mergel, J.; Stolten, D. A Comprehensive Review on PEM Water Electrolysis. *Int. J. Hydrogen Energy* **2013**, *38* (12), 4901−4934.
(35) Jouny, M.; Luc, W.; Jiao, F. General Techno-economic Analysis of CO_2 Electrolysis Systems. *Ind. Eng. Chem. Res.* **2018**, *57* (6), 2165−2177.

DOI: 10.1021/acsenergylett.9b00975
ACS Energy Lett. 2019, 4, 1427−1431